NATIONAL ADVISORY COMMITTEE FOR AERONAUTICS

WARTIME REPORT

ORIGINALLY ISSUED
September 1944 as
Advance Restricted Report L4I16

A METHOD FOR PREDICTING THE ELEVATOR DEFLECTION REQUIRED TO LAND

By R. Fabian Goranson

Langley Memorial Aeronautical Laboratory
Langley Field, Va.

NACA

WASHINGTON

NACA ARR No. L4I16

NATIONAL ADVISORY COMMITTEE FOR AERONAUTICS

ADVANCE RESTRICTED REPORT

A METHOD FOR PREDICTING THE ELEVATOR DEFLECTION REQUIRED TO LAND

By R. Fabian Goranson

SUMMARY

A method is presented for predicting from basic airplane characteristics the elevator deflection required to maintain optimum landing attitude. Charts for evaluating the components of the equation for the elevator deflection required to land, as well as a comparison of computed and measured values for 15 airplanes, are included. This comparison of experimental and computed results shows that, for preliminary design purposes, the elevator deflection required to land can be satisfactorily predicted from the basic airplane dimensions. Because of variations in piloting technique, the computed deflection is considered as the minimum value required to maintain landing attitude.

A simplified method of obtaining the downwash angle near the ground and a limited analysis of the effect of flap type and deflection on the aerodynamic-center location and pitching-moment coefficient are presented as appendixes.

INTRODUCTION

An important consideration in the horizontal-tail design is the provision of adequate elevator power to maintain optimum landing attitude. In view of this fact, flight measurements of elevator deflections used during landings were published in reference 1; however no analytical method for estimating the elevator deflection required to land was available at that time. The present study was therefore undertaken in order to develop a method by which estimates of the elevator deflection required to land could be determined from the basic dimensions of a preliminary layout.

PREDICTION OF ELEVATOR DEFLECTIONS REQUIRED TO LAND

Method of Analysis

The equilibrium equation of reference 2 has been extended by means of references 3 and 4 to include the ground effect on the downwash angle, wake location, and tail pitching moment. The ground effect on the wing and fuselage pitching moments has been neglected because available data indicate that these effects are small and inconsistent.

By considering the ground effects and solving for the elevator deflection, the equilibrium equation is

$$\delta_e = \frac{1}{\tau}\left[\epsilon - i_t - \alpha_T + \frac{-C_L S_w d + C_{m_{a.c.}} S_w \bar{c} + K_p N_p \alpha_T D^2 l_p + K_F \alpha_F w_F^2 L_F + K_F \alpha_N w_N^2 L_N N_N}{\frac{q_t}{q_o}\left(\frac{dC_{N_t}}{d\alpha_t}\right)_G l_t S_t}\right] \quad (1)$$

where basic dimensions are illustrated in figure 1 and the symbols are defined as follows with references for evaluation:

δ_e elevator deflection with respect to stabilizer, degrees; positive when trailing edge is down

τ elevator effectiveness factor (fig. 2)

$$\left(\frac{dC_{N_t}/d\delta_e}{dC_{N_t}/d\alpha_t}\right)$$

$dC_{N_t}/d\delta_e$ rate of change of horizontal-tail normal-force coefficient with elevator deflection, per degree

$dC_{N_t}/d\alpha_t$ rate of change of horizontal-tail normal-force coefficient with angle of attack at altitude, per degree (fig. 3)

A wing aspect ratio

r factor in expression for slope of normal-force curve for tail surfaces with end plates

ϵ downwash angle at elevator hinge axis, degrees (appendix A or reference 3)

i_t angle of incidence of stabilizer relative to thrust axis, degrees; positive when leading edge is up

α_T angle of attack of thrust axis with respect to relative wind, degrees; that is, sum of thrust-axis attitude at contact and $57.3\frac{w}{V}$

- w vertical velocity at contact, feet per second
- V true airspeed, feet per second

C_L lift coefficient at which airplane is operating ($Lift/q_o S_w$)

- q_o free-stream dynamic pressure, pounds per square foot

S_w wing area, including section through fuselage and ailerons, square feet

d distance, measured parallel to ground, from center of gravity to aerodynamic center of mean aerodynamic chord, feet (fig. 1); positive when aerodynamic center is behind center of gravity; aerodynamic-center location should be corrected for effect of flap deflection (appendix B)

- c chord of airfoil, feet
- b wing span, feet
- b_f flap span, feet
- d_G vertical distance from ground to root quarter-chord point of horizontal tail, feet (fig. 1)

$C_{m_{a.c.}}$ wing pitching-moment coefficient about aerodynamic center

$\bar{c}$ mean aerodynamic chord, feet

K_p empirical propeller coefficient (0.0113)

N_p number of propellers

D diameter of propeller, feet (fig. 1)

l_p distance from center of gravity to propeller plane measured parallel to thrust axis, feet (fig. 1)

K_F fuselage and engine-nacelle moment coefficient (fig. 4)

α_F angle of attack of fuselage with respect to relative wind, degrees

w_F maximum fuselage width, feet (fig. 1)

L_F over-all fuselage length, feet (fig. 1)

α_N angle of attack of nacelle with respect to relative wind, degrees

w_N maximum width of engine nacelle, feet (fig. 1)

L_N over-all length of engine nacelle, estimated to be streamline body, feet (fig. 1)

N_N number of nacelles

q_t/q_o ratio of dynamic pressure over horizontal tail to free-stream dynamic pressure (0.9 minus losses due to wake; fig. 5)

c_{d_o} section profile-drag coefficient

$\left(\frac{dc_{N_t}}{d\alpha_t}\right)_G$ slope of normal-force-coefficient curve for horizontal tail as corrected for ground effect, per degree $\left(\frac{dc_{N_t}}{d\alpha_t}\frac{c_{L_{\alpha_G}}}{c_{L_\alpha}}\right)$

$\frac{c_{L_{\alpha_G}}}{c_{L_\alpha}}$ ratio of slope of lift-coefficient curve near ground to slope of lift-coefficient curve at altitude (fig. 6; use aspect ratio and span of horizontal tail)

C_{L_α} slope of lift-coefficient curve at altitude, per degree $\left(\frac{2d_G}{b}=\infty\right)$

$C_{L_{\alpha_G}}$ slope of lift-coefficient curve near ground, per degree

l_t horizontal distance from airplane center of gravity to elevator hinge axis, feet (fig. 1)

S_t total horizontal-tail area including section through fuselage, square feet

Discussion of Components of Equation (1)

Of the various components in equation (1), one of the largest contributions to the elevator deflection required to land is the change in downwash angle as the airplane approaches the ground. Since the ground effect on the downwash angle is amply discussed in reference 3, it is sufficient to note that the decrease in downwash angle requires a substantially greater increase in the elevator deflection to maintain trim; that is, the increment of elevator deflection is equal to the change in downwash angle divided by the elevator effectiveness factor. The downwash angle near the ground may be determined by the method of appendix A or by the method of reference 3 for airplanes with tail lengths beyond the range of the charts given in appendix A. Judgment must be exercised in estimating the effect of flaps on the downwash angle because recent tests have indicated that large gaps between the flap and the fuselage may result in an upwash at the tail.

The lift characteristics of an airfoil in the presence of the ground are usually expressed in terms of a decrease in angle of attack α for a given lift coefficient. This relationship (reference 4) is expressed as

$$\Delta\alpha = -57.3\frac{C_L}{\pi A}\sigma$$

where

$$\sigma = e^{-2.48(2d_G/b)^{0.768}}$$

Since the tail moment is calculated from the tail load, the ground effect on the tail can be expressed most conveniently as an increase in the slope of the tail normal-force curve. In figure 6, the ratio of lift-curve slope near the ground to lift-curve slope at altitude is presented as a function of aspect ratio and height above the ground. These curves were plotted for a lift-curve slope of $0.10c_l$ per degree at infinite aspect ratio on the assumption that the ground effect on aspect ratio (reference 4) is

$$A_G = \frac{A}{1 - \sigma}$$

where A_G is the effective aspect ratio near the ground. Since the ground effect is expressed as a ratio of lift-curve slope near the ground to lift-curve slope at altitude, variations in lift-curve slope of the order of 10 percent from the assumed value do not materially affect the results of figure 6.

In order to evaluate correctly the horizontal-tail requirements due to the pitching moment of the wing lift about the center of gravity, the horizontal distance between the aerodynamic center and the center of gravity d must be measured at landing attitude, particularly when the vertical distance between the center of gravity and the aerodynamic center is quite large as in a high-wing monoplane. The movement of the aerodynamic center with flap deflection is also of primary importance in determining the distance d. A limited analysis of the effect of flap deflection on the aerodynamic-center location is presented in appendix B.

The usual practice of landing an airplane "tail low" often requires the horizontal tail to operate within the wing wake. The dynamic pressure may therefore be reduced below the average value of $0.9q_o$ as recommended in reference 2. The loss of dynamic pressure due to the wake may be estimated by the charts of figure 5.

As is indicated in reference 2, the propeller coefficient K_p is an empirical correction applied to bring the calculated stability criterion $d\delta_e/d\alpha$ into agreement with measured values. Using this single value of K_p gives good accuracy in estimating the propeller effects for two- or three-blade propellers but, for

high-solidity or dual-rotating propellers, it may be necessary to make a more exact evaluation by considering separately the normal forces acting on the propeller, the effect of wing upwash on the propeller, and the effect of propeller downwash on the tail. Since the entire contribution of the propeller to the elevator deflection is usually less than 2°, errors of relatively large percentage in computing the propeller effects result in negligible errors in the elevator deflection.

TEST PROCEDURE AND RESULTS

Line drawings of 15 airplanes with which landing tests have been made are shown in figure 7 and the physical characteristics of these airplanes are given in table I. Except for airplane 5, landing data obtained with airplanes 1 to 9 included phototheodolite records synchronized with NACA airspeed and control-position recorders. From the phototheodolite records, the attitude of the airplane at contact, as well as the vertical velocity during the landing approach, was obtained. For the tests in which phototheodolite records are not available, it was necessary to rely on the judgment of the pilot and an observer to choose mild three-point landings. It may be noted that all the airplanes for which data on the vertical velocity at contact are not available have a relatively high landing speed and therefore the vertical velocity attained in a normal landing would add only a small increment to the angle of attack of the thrust axis.

The data presented in reference 1 show that different landing techniques may result in wide variations (as much as 10° between the maximum and minimum values) in the elevator deflection required to land. In comparing any two landings, however, the differences in elevator deflection required to land can be credited mostly to changes in landing speed (and consequently to changes in angle of attack, lift coefficient, and downwash angle) and to differences in vertical velocity - all of which are factors considered in the present analysis.

The pitching velocity and associated damping forces, accelerations, and pitching moments due to drag forces are factors that may contribute to the elevator deflection required to land but are neglected in this analysis. The

agreement between computed and experimental elevator deflections required to land indicates that these omissions do not seriously affect the results.

COMPUTED RESULTS

In order to check the validity of the proposed method for computing the elevator deflections required to land, elevator deflections were computed for each of the airplanes of table I. A comparison of the computed and experimental results is shown in figure 8.

Wherever possible, data required to compute the elevator deflections were obtained from flight tests; thus the lift coefficient for each landing was computed from the recorded landing speed and gross weight at the time of the landing, and the angle of attack due to vertical velocity was computed from the phototheodolite records. Although such data would obviously not be available for predicting elevator deflections for a model in the preliminary design stages, the use of these data is justifiable in comparing specific computed and experimental results; that is, the comparisons in figure 8 are made for only one landing for which all flight conditions affecting the required elevator control were available and the corresponding analytical corrections were computed. The section profile-drag coefficient c_{d_o} and increment of lift coefficient due to flaps C_{L_f} were estimated from charts of reference 5. All other factors were computed by means of the charts and methods in the present report.

It is apparent from the comparison of experimental and computed elevator deflections in figure 8 that, for the propeller-idling condition, the elevator deflection required to land can be satisfactorily predicted for preliminary design purposes by the method given. Because of the effects of variations in landing technique previously discussed, the computed elevator deflection should be considered as the minimum value required to maintain the landing attitude.

A comparison of the variation with center-of-gravity location of the computed and measured elevator deflection required to land at three-point attitude is presented in figure 9 for airplane 10.

DESIGN CONSIDERATIONS

Although equation (1) presents a method for computing the elevator deflection required to land, the design application is not limited to determining the up-elevator range. Another application is the determination of the minimum ratio of elevator area to total tail area as a function of center-of-gravity location or gross weight if the elevator characteristics are known. This minimum ratio of elevator area to tail area is of particular importance because of the conflict between desirable control in flight and desirable landing control; that is, a narrow-chord elevator lessens the difficulties in obtaining light stick forces but may not be powerful enough to maintain control during a landing.

CONCLUSIONS

A method is developed for predicting from basic airplane characteristics the elevator deflection required to maintain optimum landing attitude. A comparison of results computed by this method with available experimental results indicated the following conclusions:

1. For the propeller-idling condition, the elevator deflection required to land can be satisfactorily predicted for preliminary design purposes from the basic dimensions of the airplane.

2. Because of variations in landing technique, the computed elevator deflection should be considered as the minimum value required to maintain the landing attitude.

3. The largest contribution to the elevator deflection required to land is the change in the downwash angle as the airplane approaches the ground.

Langley Memorial Aeronautical Laboratory
National Advisory Committee for Aeronautics
Langley Field, Va.

APPENDIX A

DOWNWASH ANGLES NEAR THE GROUND

By the simplified method of reference 3, the wake location has been calculated for various wing configurations and heights above the ground for tail lengths of $0.6\frac{b}{2}$, $0.8\frac{b}{2}$, and $1.0\frac{b}{2}$. These data are presented in figure 10. Straight-line interpolation between curves yields results comparable with values calculated by the method of reference 3.

Symbols used in the computation of the downwash angle that have not been previously defined are as follows:

$1/\lambda$	wing taper ratio (c_s/c_t)
c_s	root chord of wing, feet
c_t	tip chord of wing, feet
C_{L_w}	lift coefficient at particular angle of attack, flaps retracted
C_{L_f}	increase of lift coefficient, at same angle of attack, due to flap deflection
x	longitudinal distance from elevator hinge axis to quarter-chord point of root section, semispans
z	vertical distance from ground to wake origin at root section, semispans
m	vertical distance from elevator hinge axis to wake origin at root section, measured normal to relative wind (positive if hinge axis is above wake origin), semispans
h	downward displacement of center line of wake from its origin at trailing edge, measured normal to relative wind, semispans
h_o	downward displacement of wake origin from trailing edge of wing when flap is deflected, semispans

ξ longitudinal distance from elevator hinge axis to trailing edge of root section, semispans

c_f flap chord, feet; measured at root to determine ratio c_f/c_s

The downwash at the tail may be computed by the following procedure:

(1) Determine A, $1/\lambda$, b_f/b, C_{L_w}, C_{L_f}, x, z, and m. All distances (fig. 11) are measured at landing attitude in semispans parallel or perpendicular to the relative wind. The location of the wake origin with respect to the wing trailing edge h_o may be readily determined from figure 12.

(2) From figure 10, determine h_w due to plain wing.

(3) From figure 10, determine h_f due to flap.

(4) Determine net value of h by

$$h = C_{L_w} h_w + C_{L_f} h_f$$

This equation is strictly true only as long as the angles involved are small; that is,

$$\tan \epsilon_w + \tan \epsilon_f = \tan \epsilon$$

where

$$\epsilon = \epsilon_w + \epsilon_f$$

Since the downwash angle ϵ is usually less than 10°, the equation is essentially exact.

(5) From downwash charts of reference 5, determine ϵ by

$$\epsilon = C_{L_w}\left[\epsilon_w(x,\ m + h) - \epsilon_w(x,\ 2z + m - h)\right]$$

$$+ C_{L_f}\left[\epsilon_f(x,\ m + h) - \epsilon_f(x,\ 2z + m - h)\right]$$

where the subscripts of ϵ_w and ϵ_f signify that these values are to be read from the downwash charts for the plain wing and for the flap, respectively.

(6) Add wake correction of figure 13. Note that in figure 13 distances are in root chords.

(7) Subtract correction due to reflected wing wake as determined from figure 13 with height above wake center line equal to $2z + m - h$. This correction is usually very small and can be neglected.

APPENDIX B

ESTIMATION OF AERODYNAMIC-CENTER LOCATION AND PITCHING-MOMENT COEFFICIENT WITH FLAPS DEFLECTED

A limited study of the effect of flap deflection on the aerodynamic-center location and pitching-moment coefficient of NACA 230-series airfoils has been made for the airfoil-flap arrangements shown in figure 14. The aerodynamic-center location and pitching-moment coefficients were computed by the method of reference 6 from data of references 7 to 14. The results are presented in figures 15 and 16.

It must be remembered that the concept of an aerodynamic center is a device for presenting pitching-moment data in convenient form and that, particularly for airfoil-flap combinations, no point exists about which the pitching moment is constant throughout the lift range. Although only the corresponding computed pitching-moment coefficients and aerodynamic-center locations should strictly be used together, the use of faired values is permissible when the aerodynamic-center location and pitching-moment coefficient show a regular variation with flap deflection. Dashed lines are used in figure 15 to connect computed points that do not show a regular variation.

In order to expedite computation of the elevator deflection, several elaborate methods for evaluating wing pitching-moment coefficients from section data were discarded in favor of the simplified method of weighting the pitching-moment coefficient of the flapped and unflapped wing sections according to the product of the affected area and its mean aerodynamic chord. Satisfactory accuracy was obtained by assuming that the flaps affect only the flapped portion of the wing. An effective aerodynamic-center location was determined with the same assumption.

Figure 17 shows a typical wing with a partial-span flap that does not extend to the wing center line. In this arrangement, only the area blanketed by the flap is considered to be the flapped area whereas, in computing downwash angles, the flap is considered to extend to the wing center line. Although the lift

due to deflecting partial-span flaps is generally assumed to carry through the fuselage, the aerodynamic center of this additional lift apparently moves forward over the unflapped portion of the wing so that its pitching-moment coefficient (and consequently its aerodynamic center) remains nearly equal to that of the plain wing.

On this basis the weighted effective pitching-moment coefficient $C_{m_{a.c.}}$ can be expressed as

$$C_{m_{a.c.}} = \frac{S_{ctr}\bar{c}_{ctr}c_{m_{(a.c.)_o}} + S_f\bar{c}_f c_{m_{(a.c.)_f}} + S_{tip}\bar{c}_{tip}c_{m_{(a.c.)_o}}}{S_{ctr}\bar{c}_{ctr} + S_f\bar{c}_f + S_{tip}\bar{c}_{tip}} \quad (2)$$

where S is surface area, $c_{m_{a.c.}}$ is section pitching-moment coefficient with flaps retracted, and the subscripts are defined as follows:

o	plain airfoil
ctr	center portion of wing
f	flapped portion of wing
tip	tip portion of wing

When the pitching-moment coefficients in the equation (2) are replaced by the aerodynamic-center locations in percent chord, a weighted effective aerodynamic-center location in percent of the wing mean aerodynamic chord is obtained.

The mean aerodynamic chord may be approximated with sufficient accuracy by

$$\bar{c} = \frac{2}{3}\left(c_s + c_t - \frac{c_s c_t}{c_s + c_t}\right)$$

$$= \frac{2}{3}c_s\left(1 + \frac{\lambda^2}{1 + \lambda}\right)$$

REFERENCES

1. Vensel, Joseph R.: Flight Measurements of the Elevator Deflections Used in Landings of Several Airplanes. NACA ARR, Nov. 1941.

2. Gilruth, R. R., and White, M. D.: Analysis and Prediction of Longitudinal Stability of Airplanes. NACA Rep. No. 711, 1941.

3. Katzoff, S., and Sweberg, Harold H.: Ground Effect on Downwash Angles and Wake Location. NACA Rep. No. 738, 1943.

4. Wetmore, J. W., and Turner, L. I., Jr.: Determination of Ground Effect from Tests of a Glider in Towed Flight. NACA Rep. No. 695, 1940.

5. Silverstein, Abe, and Katzoff, S.: Design Charts for Predicting Downwash Angles and Wake Characteristics behind Plain and Flapped Wings. NACA Rep. No. 648, 1939.

6. Thompson, M. J.: A Simple Method for Determining the Aerodynamic Center of an Airfoil. Jour. Aero. Sci., vol. 5, no. 4, Feb. 1938, pp. 138-140.

7. Abbott, Ira H., and Greenberg, Harry: Tests in the Variable-Density Wind Tunnel of the N.A.C.A. 23012 Airfoil with Plain and Split Flaps. NACA Rep. No. 661, 1939.

8. Wenzinger, Carl J., and Harris, Thomas A.: Wind-Tunnel Investigation of an N.A.C.A. 23012 Airfoil with Various Arrangements of Slotted Flaps. NACA Rep. No. 664, 1939.

9. Wenzinger, Carl J., and Harris, Thomas A.: Wind-Tunnel Investigation of N.A.C.A. 23012, 23021, and 23030 Airfoils with Various Sizes of Split Flap. NACA Rep. No. 668, 1939.

10. Wenzinger, Carl J., and Harris, Thomas A.: Wind-Tunnel Investigation of an N.A.C.A. 23021 Airfoil with Various Arrangements of Slotted Flaps. NACA Rep. No. 677, 1939.

11. Harris, Thomas A.: Wind-Tunnel Investigation of an N.A.C.A. 23012 Airfoil with Two Arrangements of a Wide-Chord Slotted Flap. NACA TN No. 715, 1939.

12. Duschik, Frank: Wind-Tunnel Investigation of an N.A.C.A. 23021 Airfoil with Two Arrangements of a 40-Percent-Chord Slotted Flap. NACA TN No. 728, 1939.

13. Lowry, John G.: Wind-Tunnel Investigation of an NACA 23012 Airfoil with Several Arrangements of Slotted Flaps with Extended Lips. NACA TN No. 808, 1941.

14. Harris, Thomas A., and Purser, Paul E.: Wind-Tunnel Investigation of an NACA 23012 Airfoil with Two Sizes of Balanced Split Flap. NACA ACR, Nov. 1940.

TABLE I

PHYSICAL CHARACTERISTICS OF 15 AIRPLANES TESTED AND CONDITIONS EXISTING IN LANDINGS USED IN FIGURE 8

Airplane	Symbol	Wing area (sq ft)	Wing span (ft)	Wing aspect ratio	Wing taper ratio	Flap type	Flap deflection (deg)	$\bar{c}$ (ft)	c.g. (percent $\bar{c}$)	d (ft)	Height of wake origin, z (b/2)	d_G (ft)	Tail area (sq ft)	Tail span (ft)	Tail aspect ratio	S_e/S_t	i_t (deg)	Gross weight (lb)	Landing speed (mph)	w (fps)	α_T (deg)
1	○	169	36	7.7	1:1	None	0	4.68	27.9	0.18	0.27	1.78	25.2	10.2	4.1	0.46	-4	1,090	52.7	0.8	10.4
	Q						0			.22									51.5	3.5	11.6
2	+	180	36	7.2	1:1	None	0	4.98	25.1	.13	.28	2.2	26	10.0	3.9	.42	3	1,058	37.9	.7	9.1
3	×	155	34	7.5	1:1	Slotted	30	4.75	28.7	.20	.30	1.58	28	9.3	3.1	.39	0	1,373	46.8	.9	11.3
4	□	236	37.3	5.9	2.5:1	Split	30	6.8	26.7	-.04	.13	2.75	48	12.8	3.4	.40	2	5,750	69.4	1.6	12.6
	□						45			.01	.12								73.3	.9	12.1
5	◇	248	42	7.1	1.8:1	Split	0	6.05	23.0	.07	.08	2.68	48	13.0	3.5	.425	0	4,440	66	---	12.0
	◇						20			.19	.07								66	---	12.0
6	△	1420	104	7.6	2.7:1	Split	0	14.8	29.1	-.78	.09	3.5	254	33.8	4.5	.37	0	38,600	94	1.2	8.1
	△						30			-.53	.07								87	4.4	6.9
	△						60			-.37	.05								83	2.1	8.7
7	▽	2780	149	8.0	4.3:1	Split	25	21.3	25.9	-.08	.04	4.05	505	45	4.0	.36	0	48,100	69.7	2.1	7.6
8	◸	602	65	7	3:1	Slotted	35	10.15	20.9	.45	.21	5.74	118	23.7	4.75	.35	1	27,586	116	1	9.0
9	◹	162	34	7.2	2:1	None	0	4.96	22.0	-.10	.17	2.3	25.1	10.8	4.7	.38	-3	1,340	61.3	.7	10.9
10	◺	236	37	5.8	2.1:1	Plain	50	6.64	23.8	.14	.20	3.25	31.2	13.2	3.8	.45	2	7,274	84	---	11.2
11	◿	258	39	5.9	1.5:1	Split	67	6.94	25.6	.06	.18	2.25	61.2	14.8	3.6	.5	0	5,514	71	---	10.5
12	▷	258	40	6.2	2:1	Split	80	7.03	27.1	-.02	.13	3.3	37.1	11.0	3.3	.35	2	7,014	70	---	10.7
13	◁	260	38	5.6	1.7:1	Split	40	7.01	28.5	-.16	.17	3.84	49	13.7	3.85	.38	-1.5	6,566	78	---	9.7
14	⋈	236	37.5	5.9	2.3:1	Split	45	6.80	31.2	-.30	.12	3.5	48.3	12.8	3.4	.28	2	8,100	80	---	10.8
15	⊞	300	40.1	5.6	Elliptical	Slotted	40	7.28	28.0	0	.10	2.92	584	16.0	4.4	.31	1.5	11,809	102	---	10.5

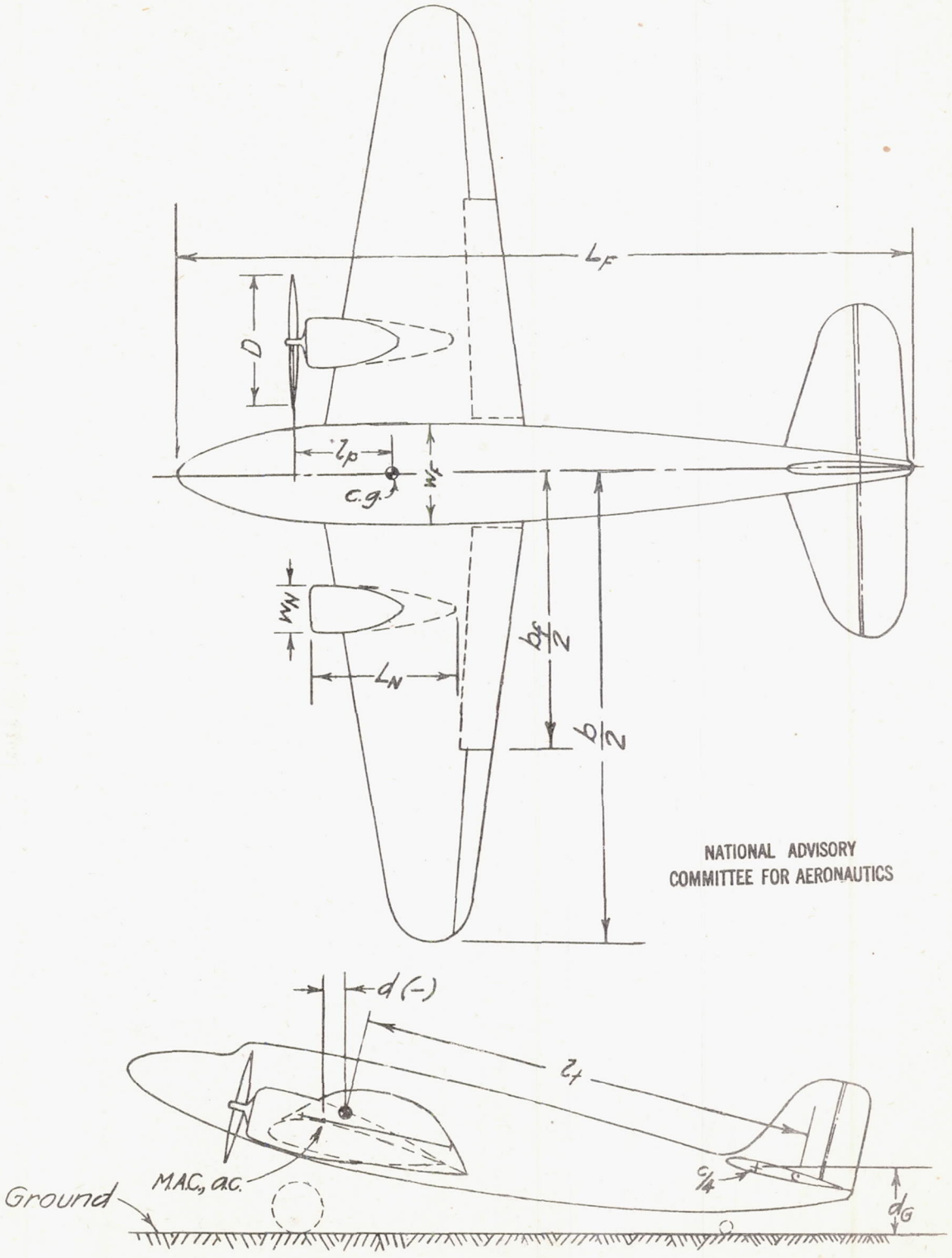

Figure 1.- Basic dimensions used in calculating elevator deflection required to land.

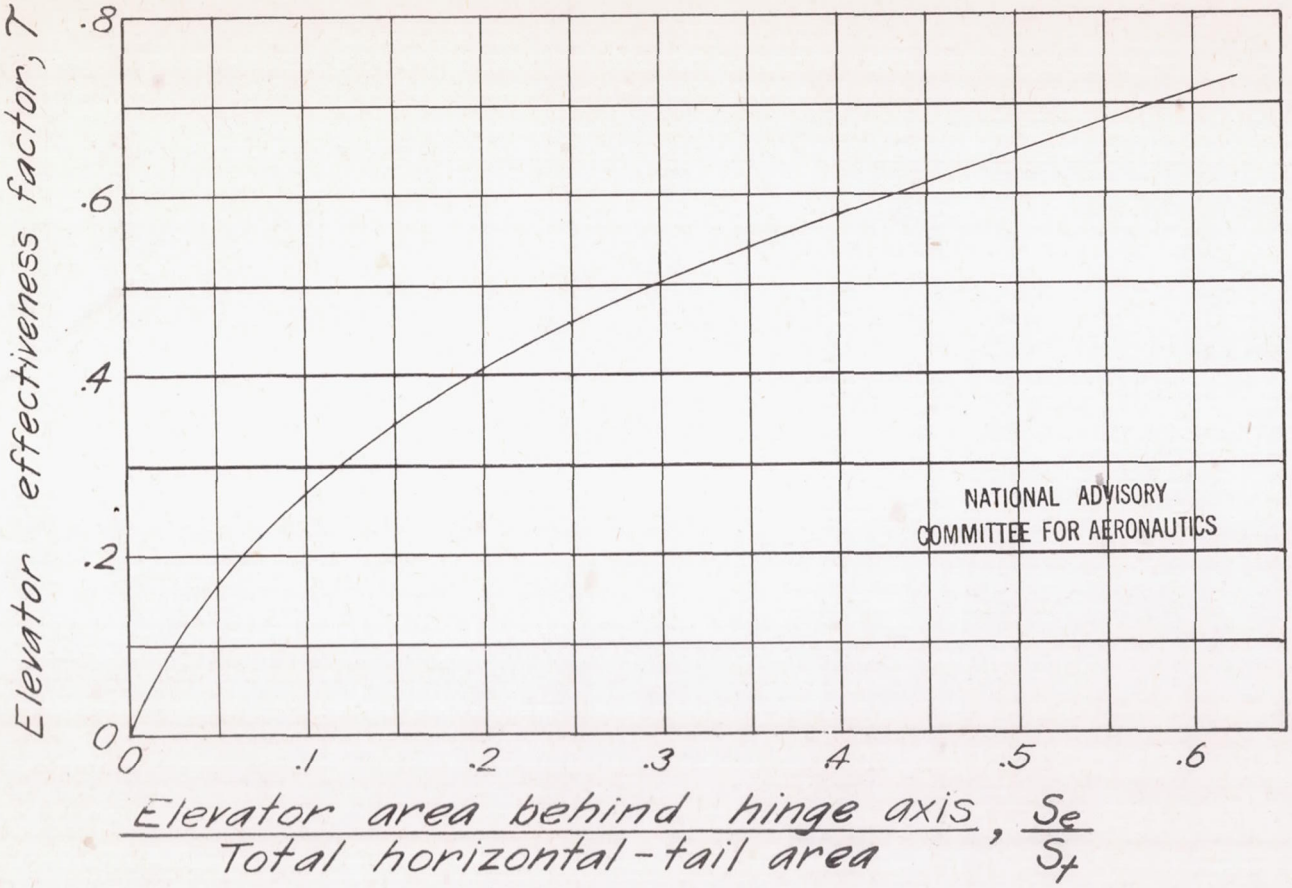

Figure 2.- Variation of elevator effectiveness factor τ with ratio of elevator area behind hinge axis to total horizontal-tail area. (From reference 2.) $\tau = \frac{dC_{N_t}/d\delta_e}{dC_{N_t}/d\alpha_t}$.

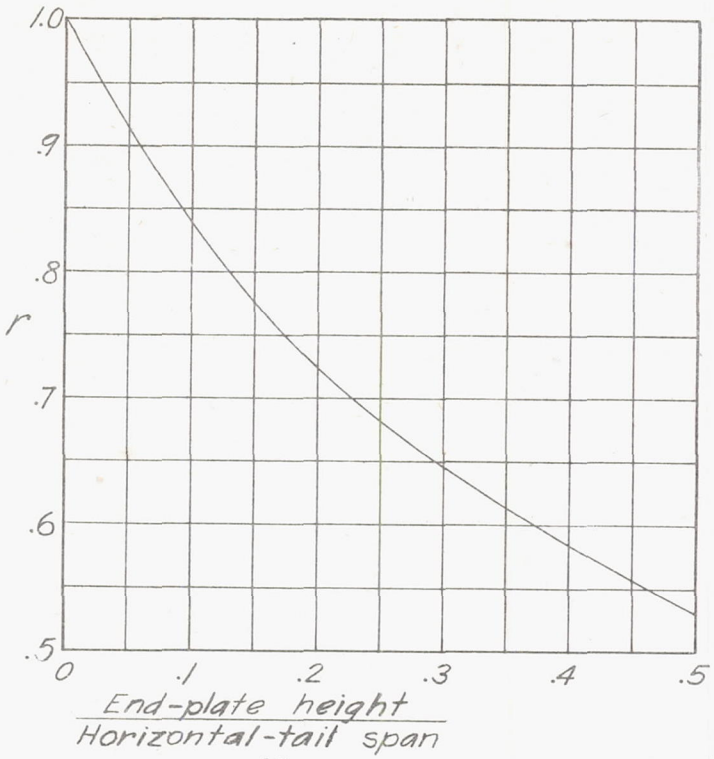

(a) Correction to $\frac{dC_{N_t}}{d\alpha_t}$ for end-plate effect; $\frac{dC_{N_t}}{d\alpha_t} = \frac{0.01}{1 + 1.8\frac{r}{A}}$.

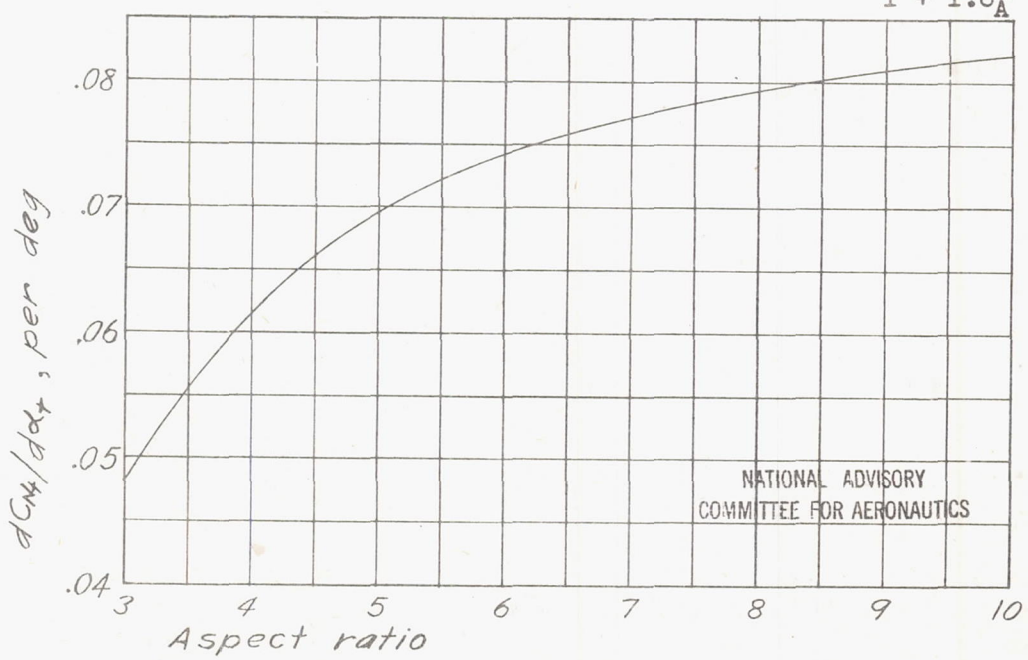

(b) Without end plates.

Figure 3.- Variation of $\frac{dC_{N_t}}{d\alpha_t}$ with aspect ratio for conventional sections. (From reference 2.)

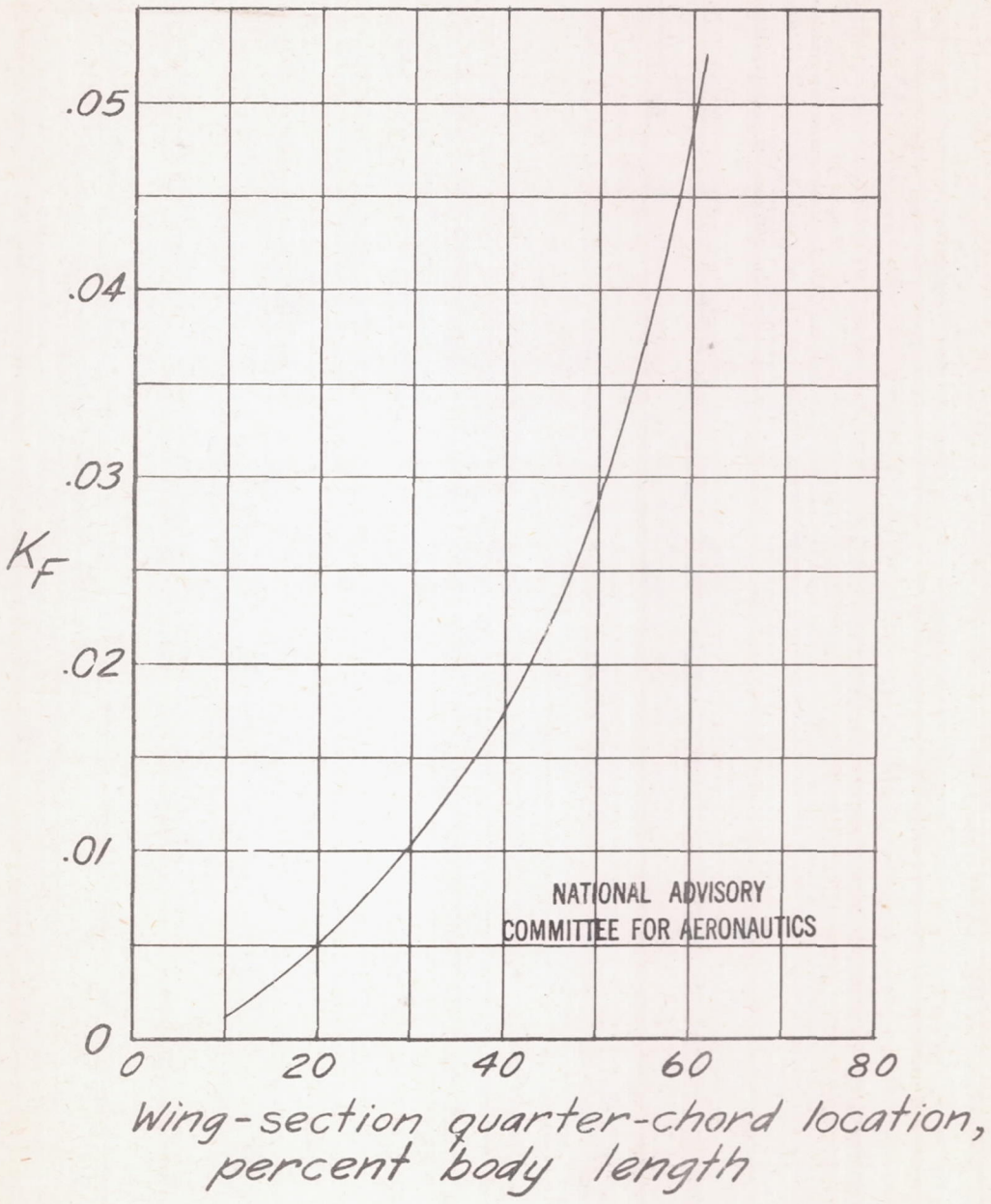

Figure 4.- Variation of fuselage and engine-nacelle moment coefficient K_F with relative location of wing and body. Wing root chord used to obtain fuselage factor and local wing chord to obtain nacelle factors. (From reference 2.)

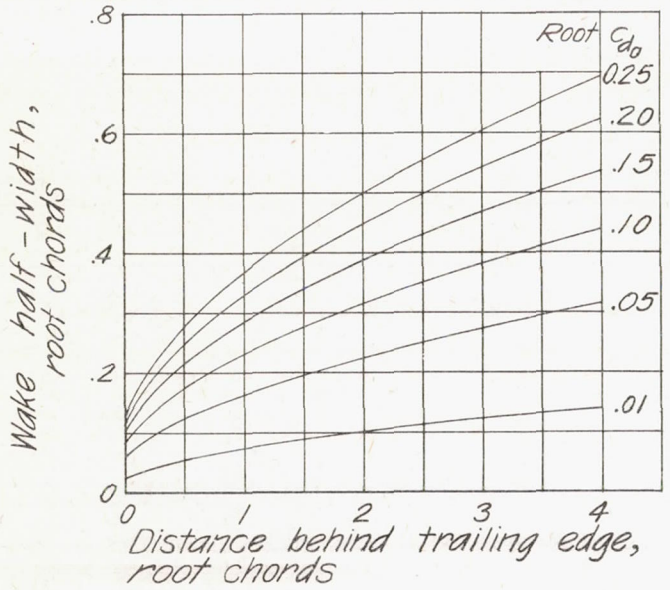

(a) Variation of wake width with distance from trailing edge.

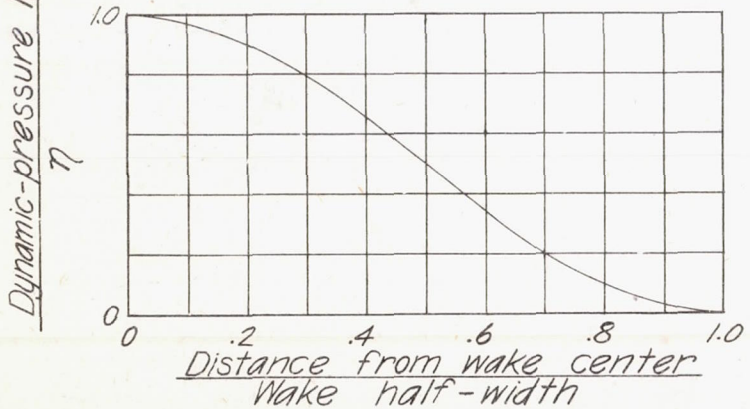

(b) Variation of dynamic pressure across wake.

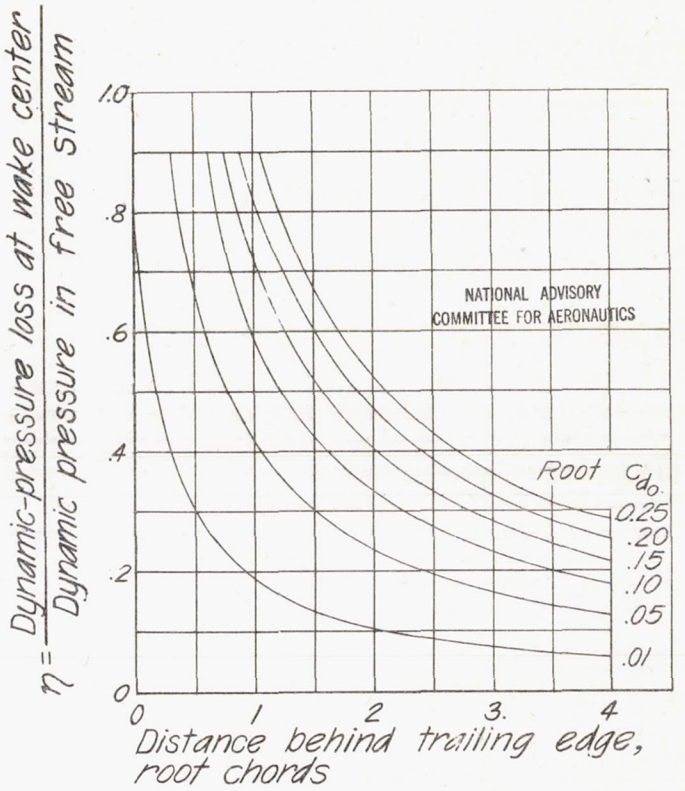

(c) Relation between maximum loss of dynamic pressure in wake and distance behind trailing edge.

Figure 5.- Effect of wake on dynamic pressure at tail q_t. (From reference 5.)

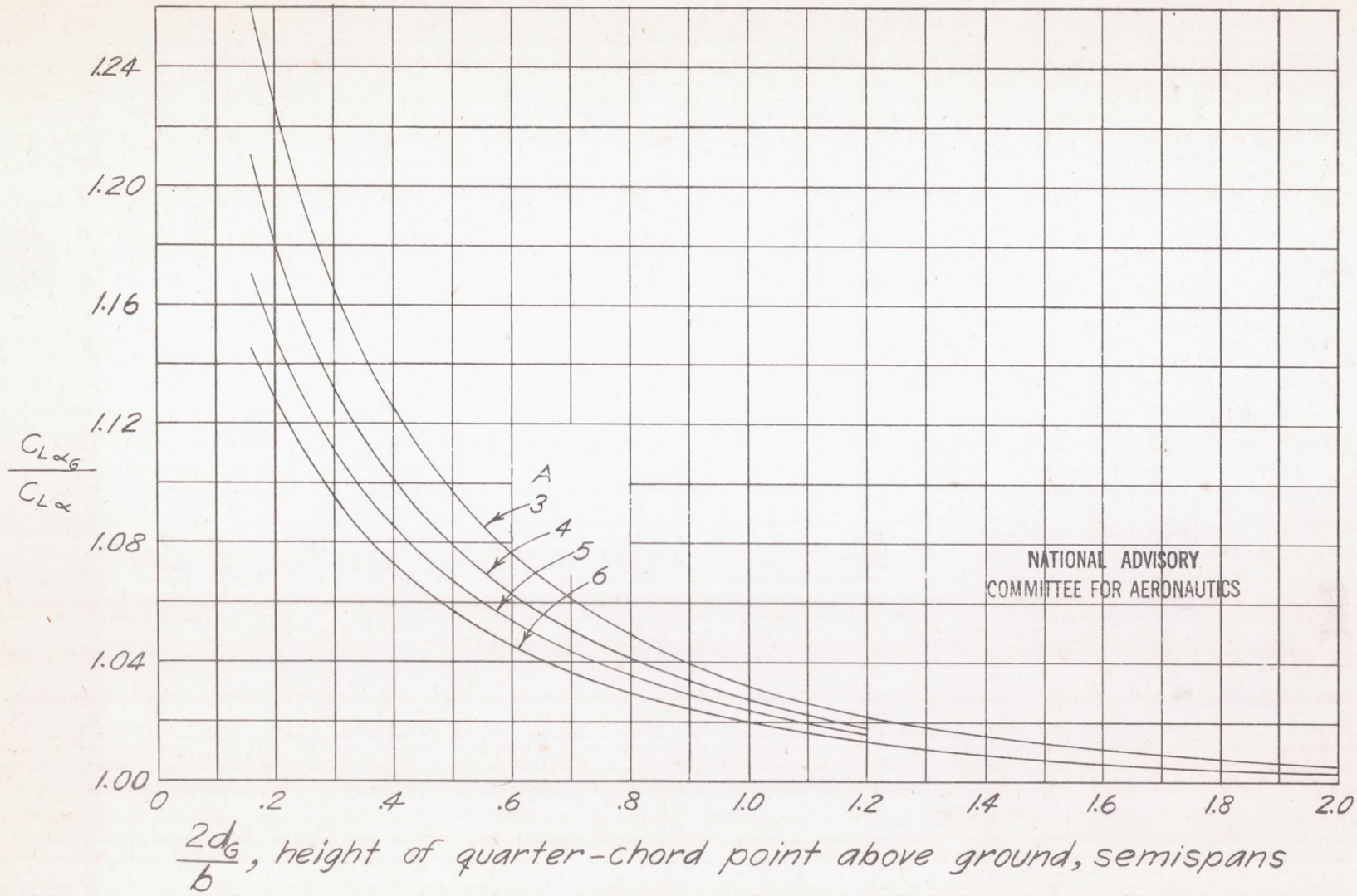

Figure 6.- Ground effect on lift-curve slope.

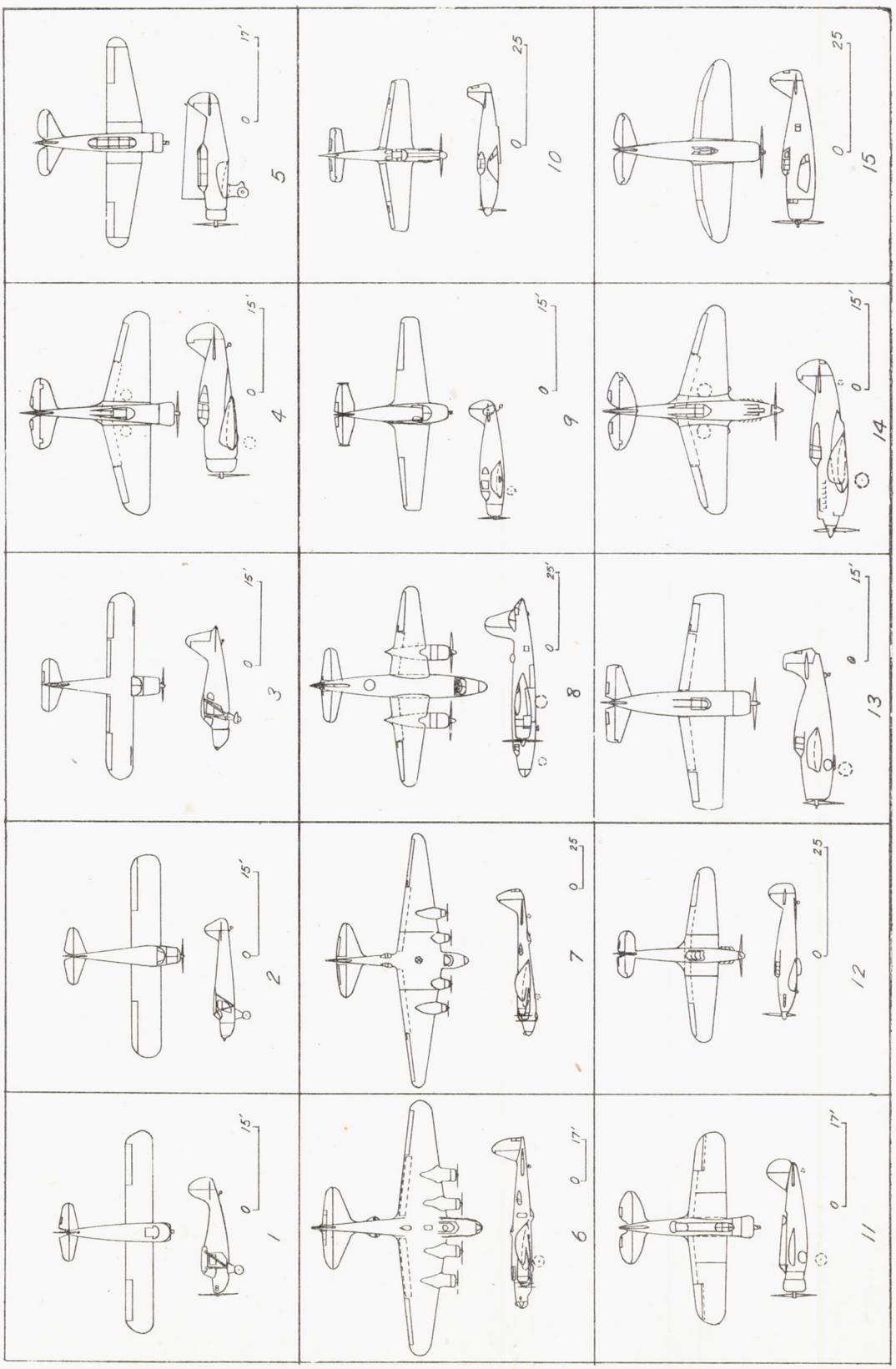

Figure 7.- Airplanes tested in landing.

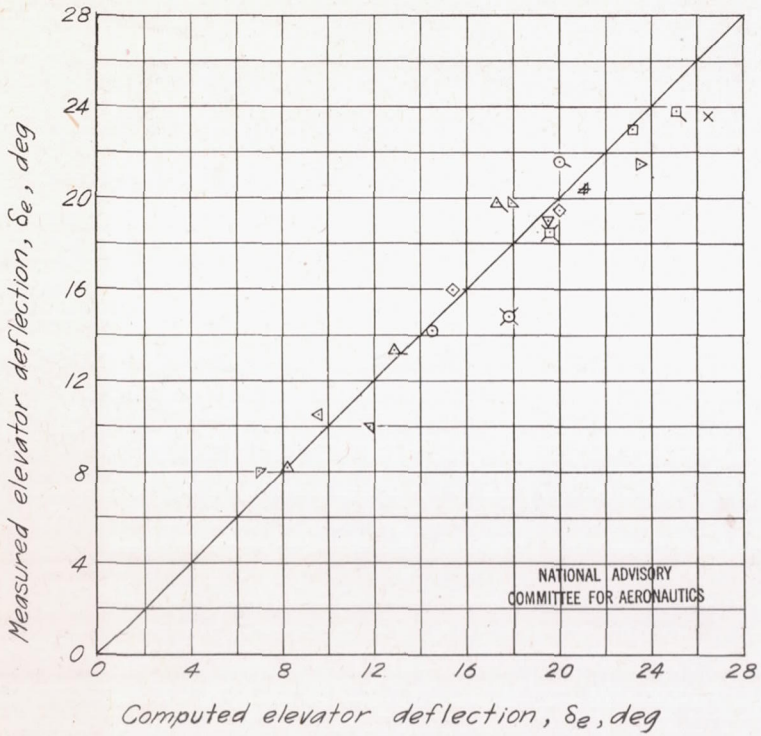

Figure 8.- Comparison of flight measurement of elevator deflection required to land with computed values. Symbols from table I.

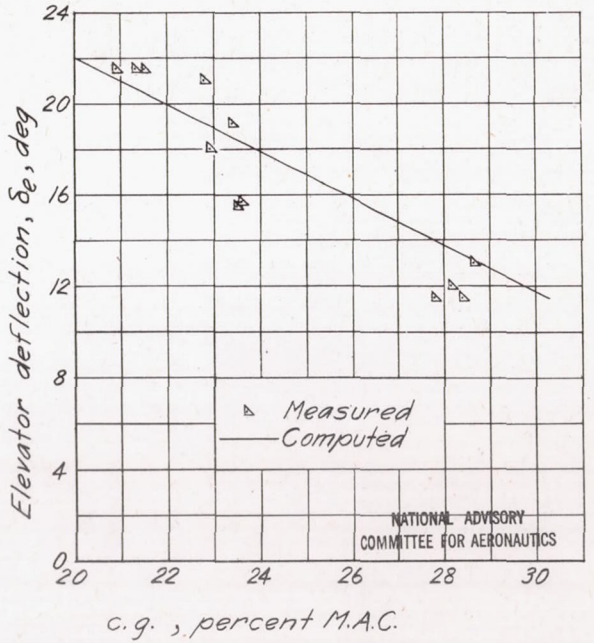

Figure 9.- Variation with center-of-gravity location of elevator deflection required to land at three-point attitude for airplane 10.

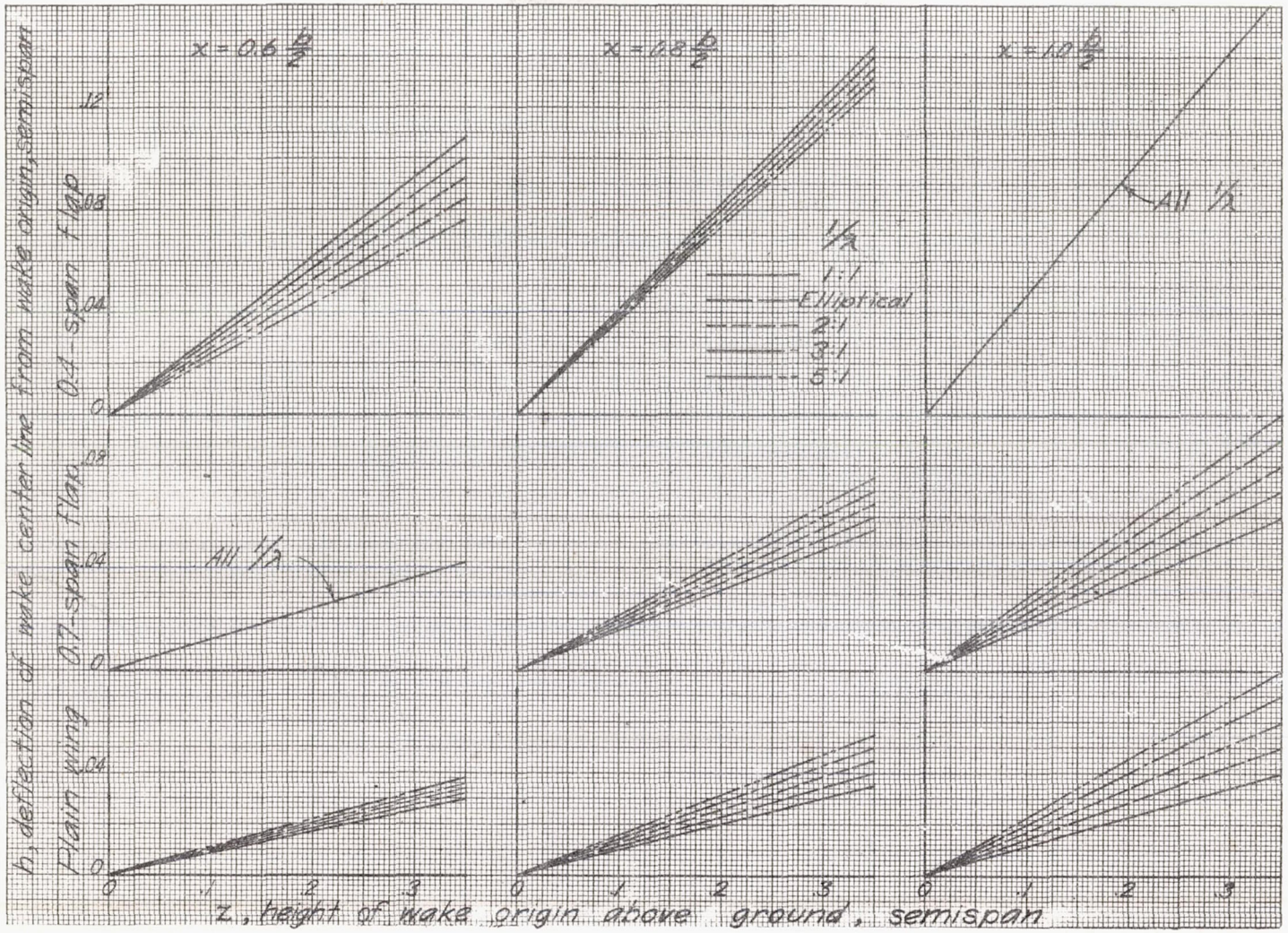

(a) A = 6, C_{L_w} = 1.0, C_{L_f} = 1.0.

NATIONAL ADVISORY
COMMITTEE FOR AERONAUTICS

Figure 10.- Wake center-line deflection near the ground.

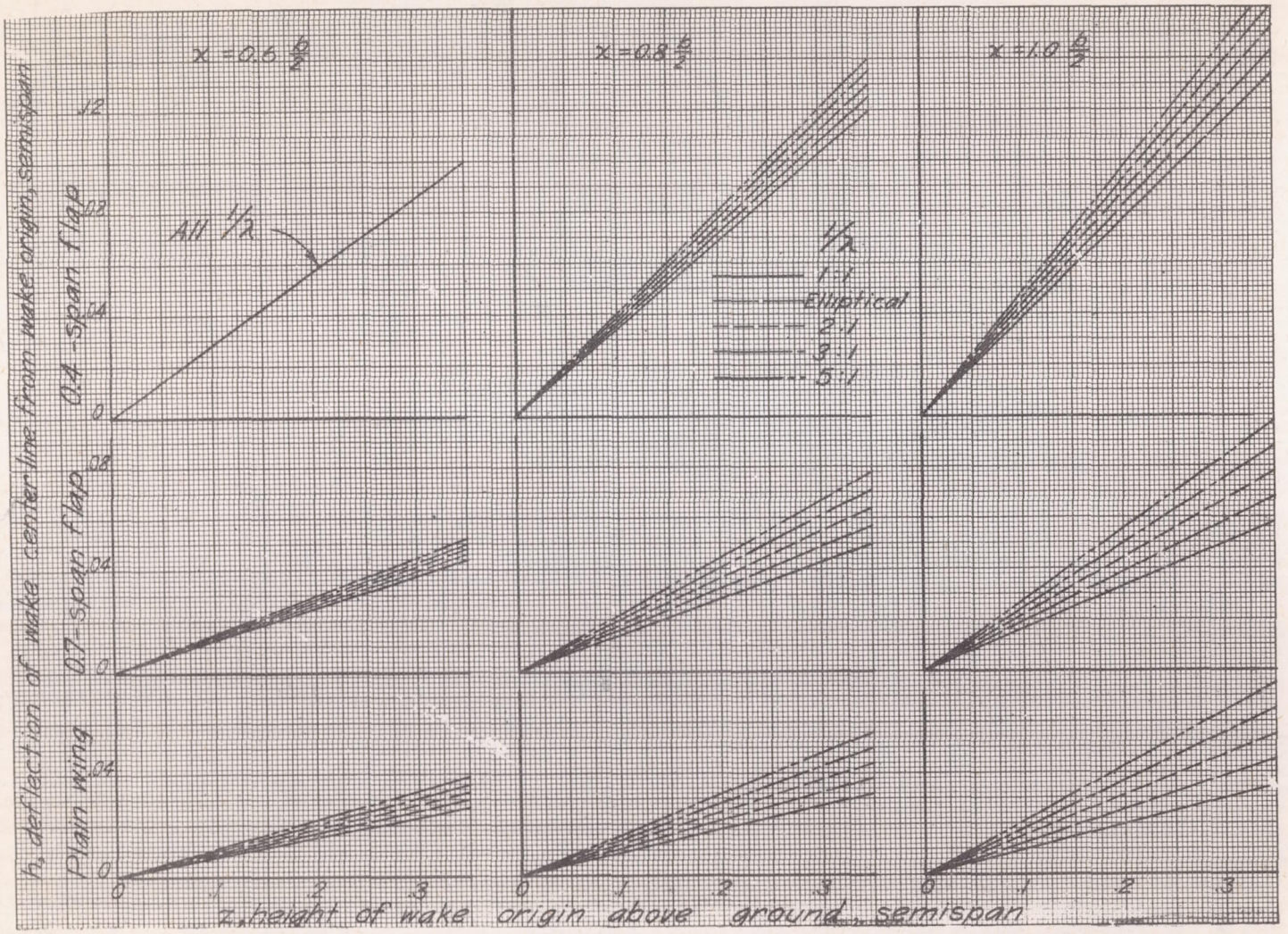

(b) A = 9, C_{L_w} = 1.0, C_{L_f} = 1.0.

NATIONAL ADVISORY COMMITTEE FOR AERONAUTICS

Figure 10.- Continued.

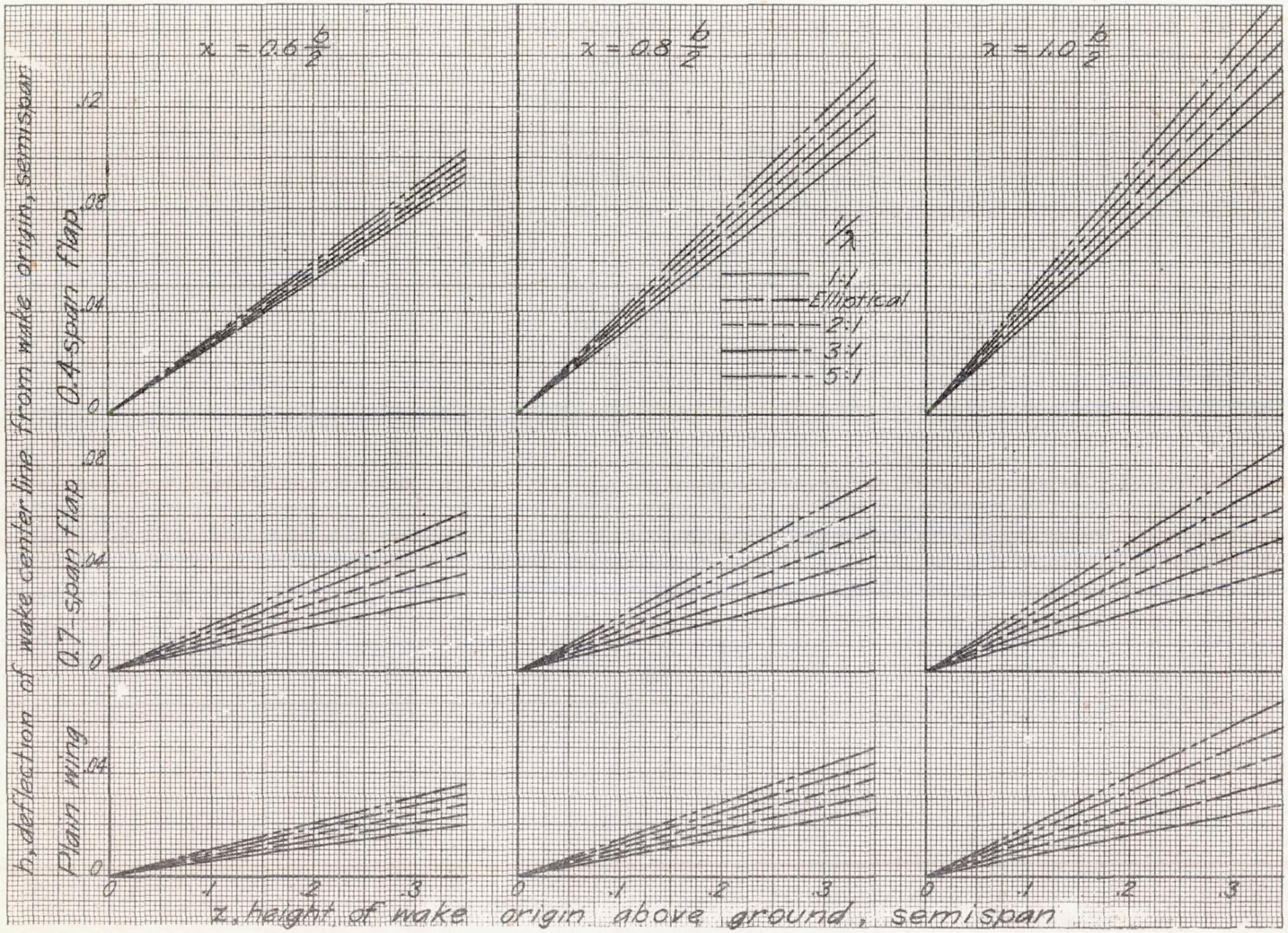

(c) A = 12, C_{L_w} = 1.0, C_{L_f} = 1.0.

NATIONAL ADVISORY
COMMITTEE FOR AERONAUTICS

Figure 10.- Concluded.

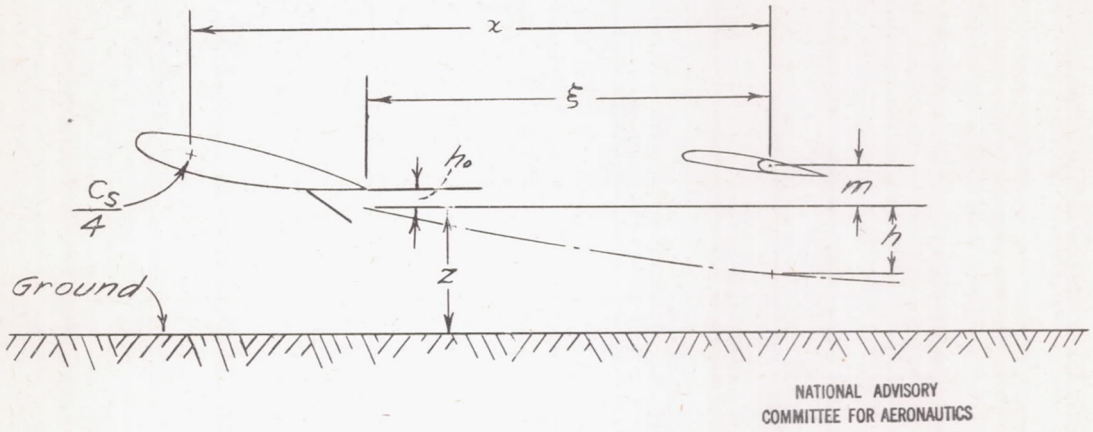

Figure 11.- Distances, measured at plane of symmetry, used in determining wake location and downwash angle.

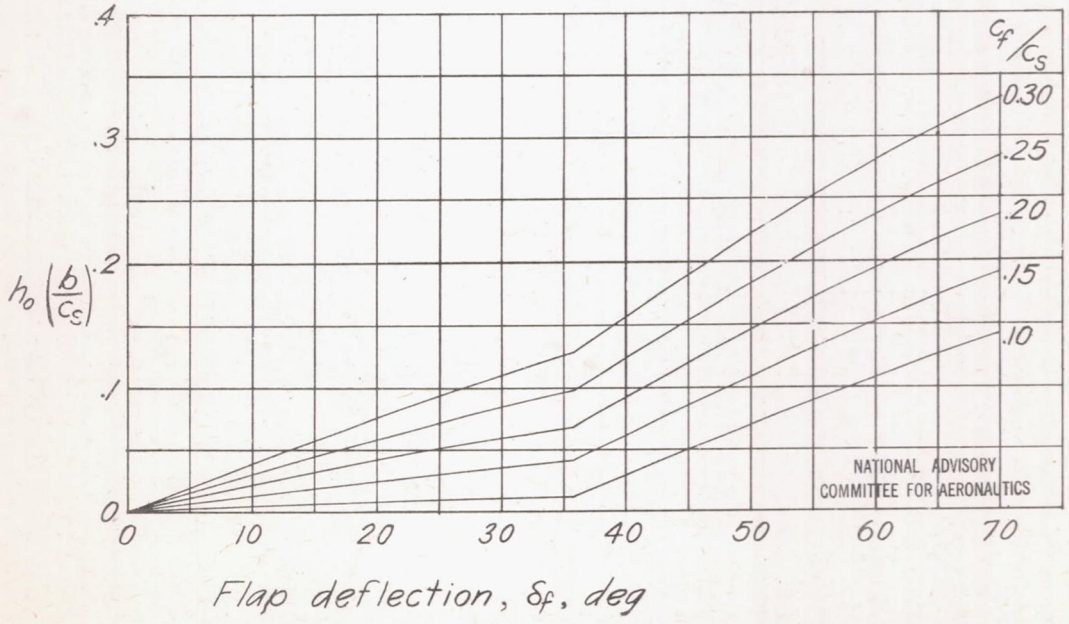

Figure 12.- Downward displacement of wake origin as a function of flap deflection. (Data from reference 5.)

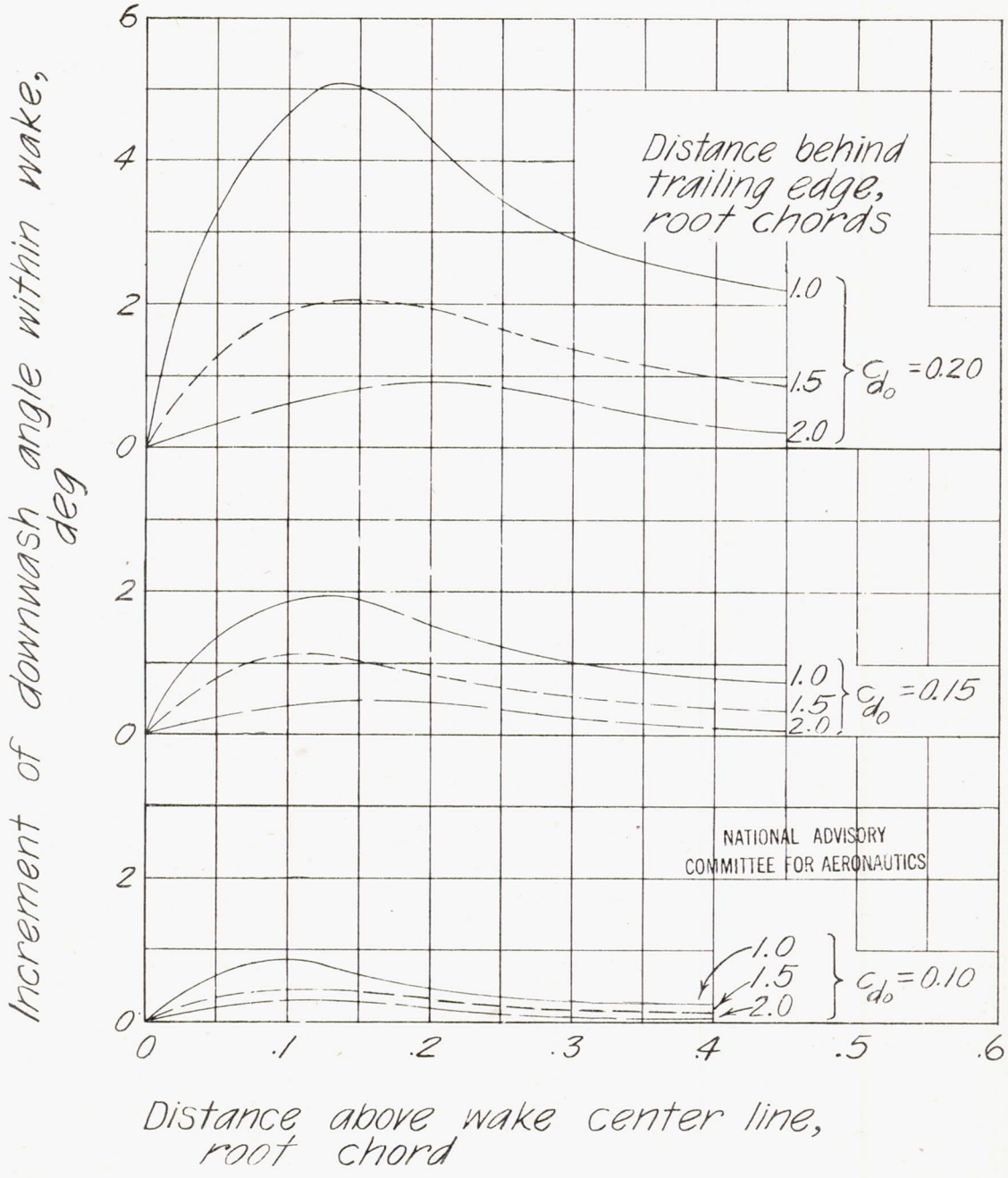

Figure 13.- Wake effect on downwash. Effects equal but of opposite sign below wake center. (From reference 3.)

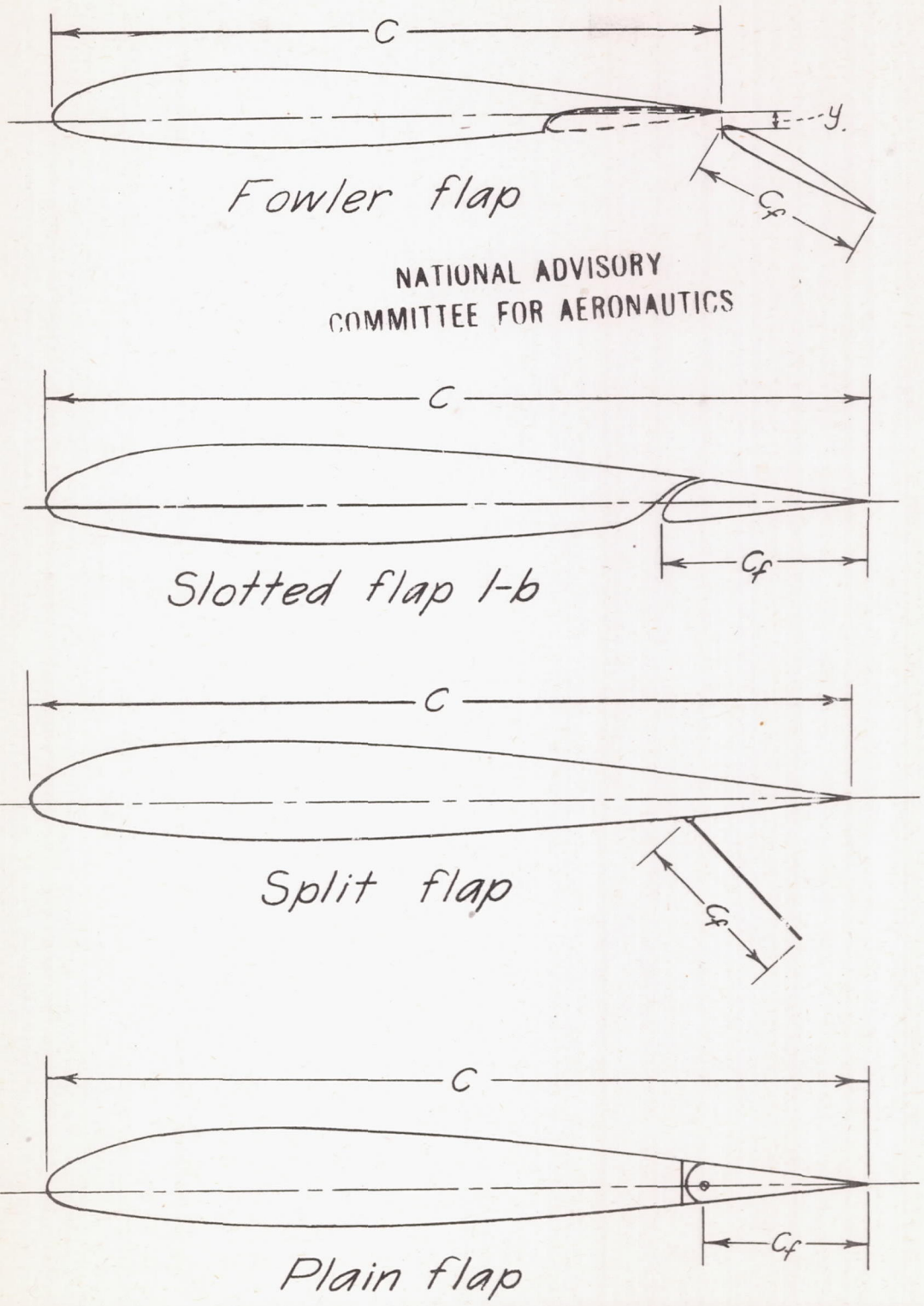

Figure 14.- Airfoil-flap combinations investigated.

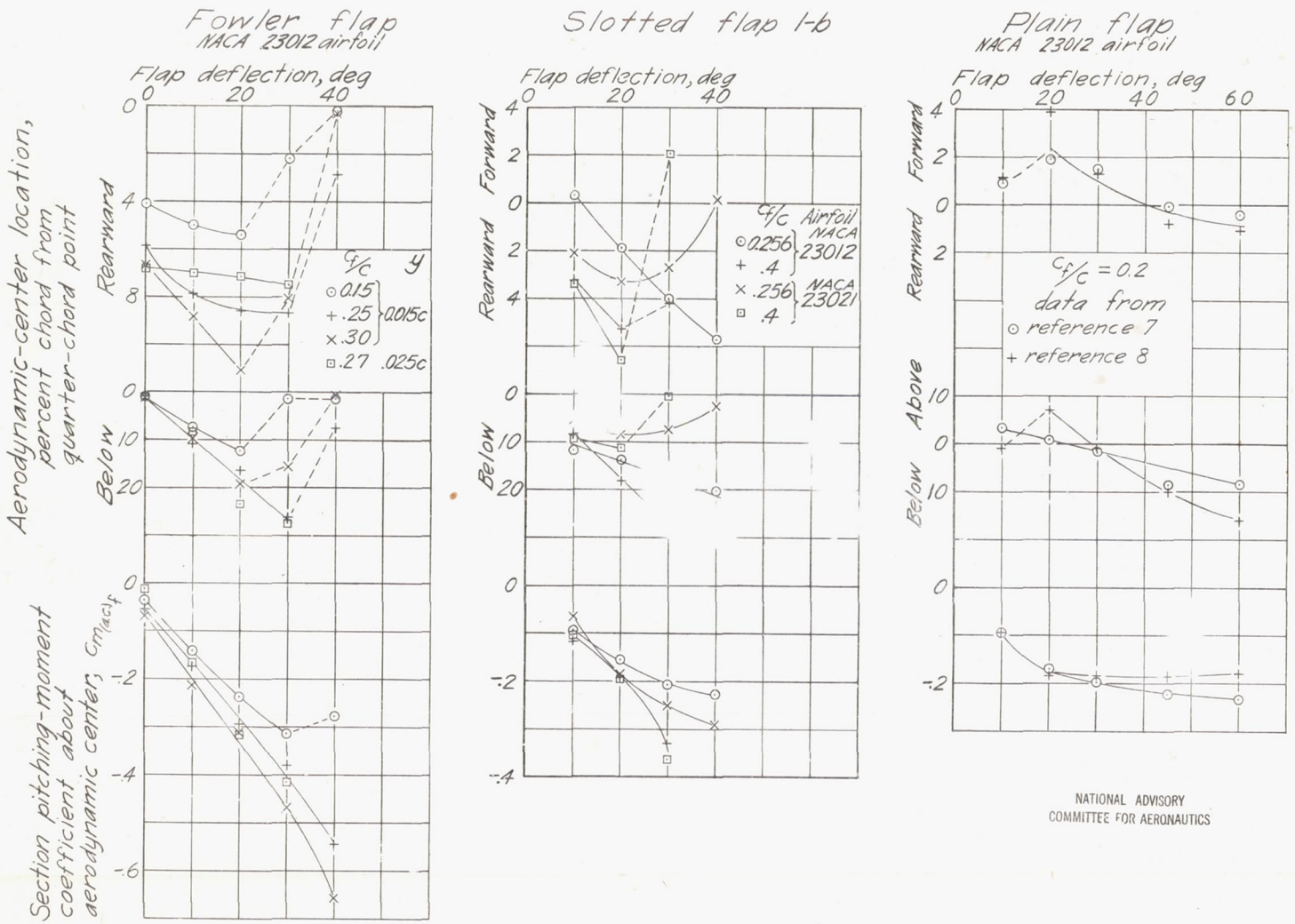

(a) Effect of various flap types on NACA 23012 airfoil.

Figure 15.- Effect of flap deflection on aerodynamic-center location and pitching-moment coefficient for various flap types on NACA 230-series airfoils.

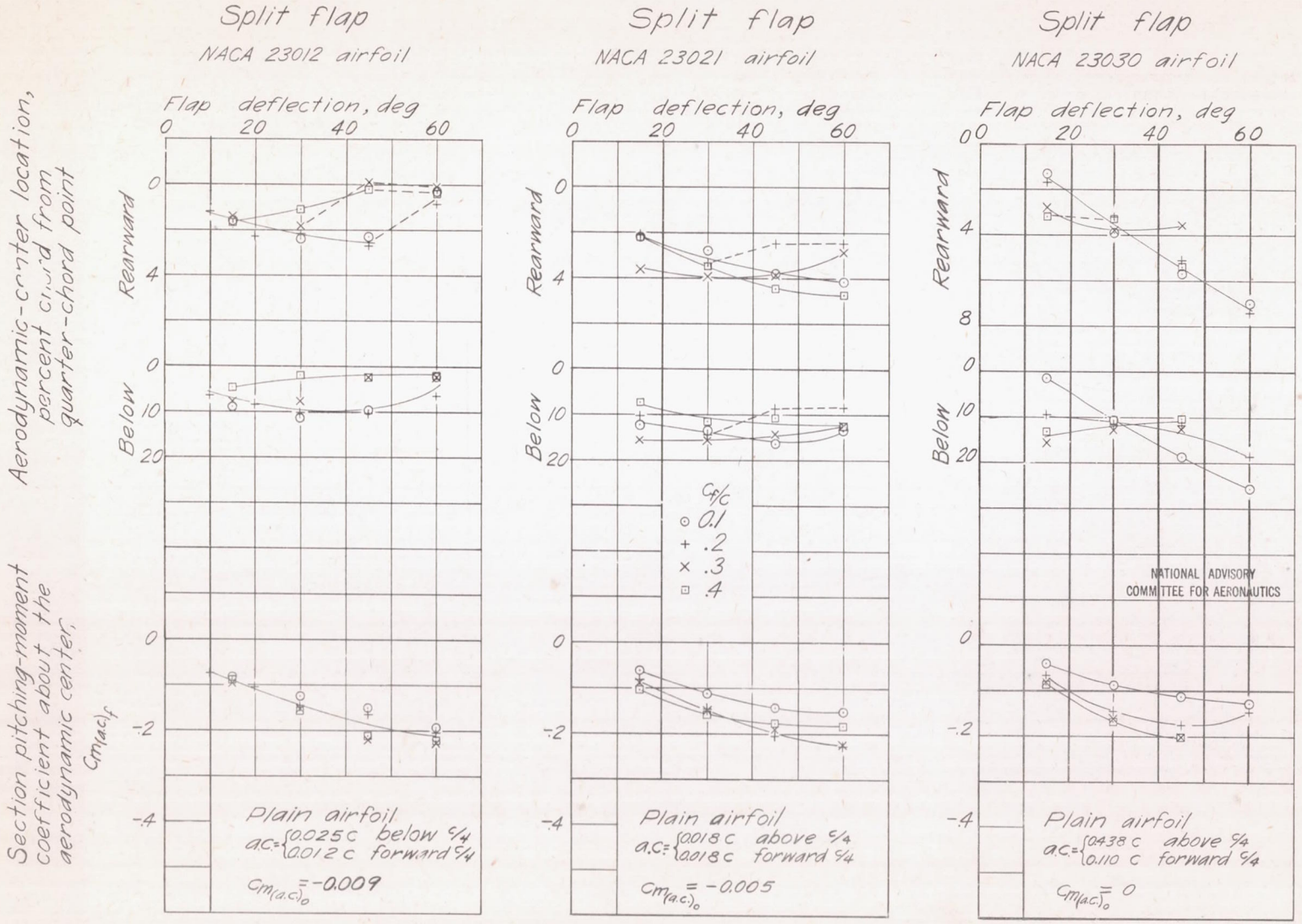

(b) Effect of airfoil thickness with a split flap.

Figure 15.- Concluded.

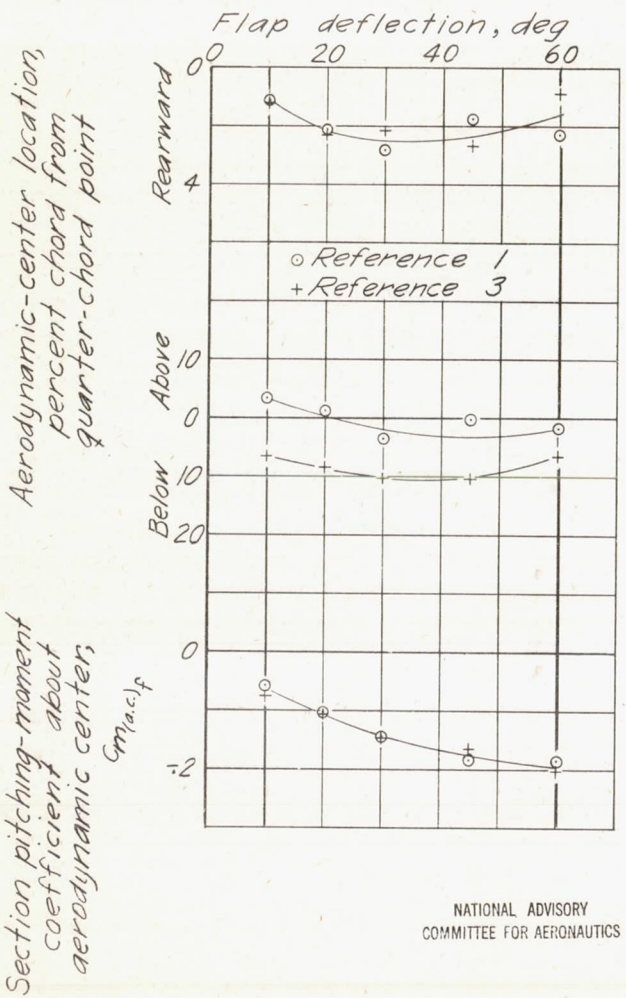

Figure 16.- Variation in aerodynamic-center location indicated by tests in different wind tunnels for split flap on NACA 23012 airfoil. $\frac{c_f}{c} = 0.2$.

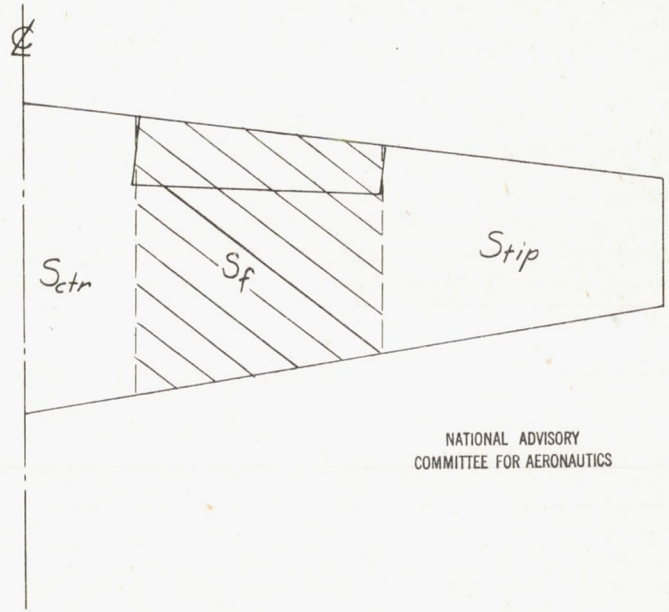

Figure 17.- Distribution of areas for calculating effective aerodynamic-center location and pitching-moment coefficient of a typical partial-span flap.